Efficient enrichment of nickel and iron in laterite nickel ore by deep reduction and magnetic separation

Shuai YUAN, Wen-tao ZHOU, Yan-jun LI, Yue-xin HAN

College of Resources and Civil Engineering, Northeastern University, Shenyang 110819, China

Abstract: The process of deep reduction and magnetic separation was proposed to enrich nickel and iron from laterite nickel ores. Results show that nickel–iron concentrates with nickel grade of 6.96%, nickel recovery of 94.06%, iron grade of 34.74%, and iron recovery of 80.44% could be obtained after magnetic separation under the conditions of reduction temperature of 1275 °C, reduction time of 50 min, slag basicity of 1.0, carbon-containing coefficient of 2.5, and magnetic field strength of 72 kA/m. Reduction temperature and time affected the possibility of deep reduction and reaction progress. Slag basicity affected the composition of slag in burden and the spilling and enriching rate of nickel–iron from a matrix to form nickel–iron particles. Nickel–iron particles were generated, aggregated, and grew gradually in the reduction process. Nickel–iron particles can be effectively separated from gangue minerals by magnetic separation.

Key words: laterite nickel ore; deep reduction; magnetic separation; nickel–iron concentrate; reduction mechanism

1 Introduction

Nickel is important to the national economy owing to its high mechanical strength, ductility, chemical stability, and corrosion resistance [1−3]. In China, nickel sulfide ores have long been used as a raw material for nickel production; the difficulty of its resource exploitation is increasing with the decrease of reserves. Therefore, laterite nickel ores, which constitute 72.2% of the world's land-based nickel reserves, have attracted significant attention from nickel producers and stainless steel enterprises owing to their rich reserves, easy exploitation, and mature smelting process [4,5].

Recently, many experts and scholars have developed and applied different technological methods according to the different characteristics of laterite nickel ores [6−8]. The typical pyro-metallurgical process is the rotary kiln-electric furnace reduction smelting process, which is a pyrometallurgical process widely used in laterite nickel ore smelters. When handling laterite nickel ores with high copper and cobalt contents, a wet process is more conducive to the comprehensive recovery of various valuable metals and the reduction in energy consumption. Currently, only the Nippon Yakin Oheyama Smelter of Japan Metallurgical Company combines pyrometallurgical and hydrometallurgical processes to treat nickel oxides [9]. Although the Nippon Yakin Oheyama Smelter has been improved many times, the technology is still unstable. Nickel and cobalt leaching from laterite nickel ores is a serious issue, especially in the application of fungi in the bio-leaching [10,11]. In addition, other treatment processes of low-grade laterite nickel ores have been extensively studied, primarily including chlorination separation−magnetic separation, reduction sulfide roasting−magnetic separation, and

Corresponding author: Wen-tao ZHOU; Tel: +86-13840541273; E-mail: 13840541273@163.com

direct reduction and magnetic separation [12−14]. WANG et al [15] achieved the recoveries of Ni and Fe of 75.70% and 77.97%, respectively, at 1500 °C and reduction time 90 min using direct reduction and magnetic separation technology; TANG et al [16] achieved recoveries of Ni and Fe of 84.38% and 53.76%, respectively, in the temperature range from 700 to 1000 °C. It is clear that temperature significantly affected direct reduction and magnetic separation. Although some achievements have been made in the laboratory, owing to the effect of industrial equipment and production scale, no industrial test has been performed. The cost of wet treatment is lower than that of pyrometallurgical treatment, but the treatment process of nickel oxide ores is more complex and requires higher technological conditions. Bioleaching involves low environmental pollution and low cost, but its leaching cycle is long, and it is not yet mature for industrial production. In summary, the thermometallurgical treatment of nickel oxide ores for producing ferronickel exhibits the characteristics of short process, high efficiency, and high energy consumption. Currently, pyro-metallurgical processes are primarily designed for high-grade laterite nickel ores [17,18].

Owing to environmental pollution, long process flow, high requirement for equipment, and high energy consumption in the wet process, a "deep reduction and magnetic separation" process was proposed in this study to enrich nickel and iron from laterite nickel ores, which used coal powder as a reducing agent to reduce laterite nickel ores to metallic iron and nickel at a temperature lower than the ore melting temperature. By adjusting and promoting the aggregation and growth of metal iron and nickel into a certain size of iron particles, iron and nickel powder could be obtained by the efficient separation of reduced materials [19]. Deep reduction was a state between "direct reduction" and "smelting reduction". The method included two processes: iron nickel oxide reduction and iron nickel particle growth. First, nickel minerals and iron ores in laterite nickel ores were reduced to nickel–iron metal particles by deep reduction, and then the reduction materials were separated by magnetic separation. Meanwhile, chemical analysis, X-ray diffraction (XRD), scanning electron microscopy (SEM), and energy dispersive spectrometry (EDS) were used to systematically

study the chemical composition, mineral composition and micro-morphology of deep reduction materials, respectively.

2 Experimental

2.1 Materials

The low-grade laterite ore used in this experiment was from a mine in Myanmar. The chemical composition and nickel phases of the raw materials are presented in Tables 1 and 2, respectively. The mineralogical phase was determined by XRD, as shown in Fig. 1. The low-grade laterite ore comprised 2.26% Ni, 14.24% total Fe, 41.41% SiO_2, 17.24% MgO and 1.99% Al_2O_3. The nickel used primarily existed in the form of nickel silicate and could not be reclaimed by conventional methods. The results in Fig. 1 indicate that the major mineral phases were nickeliferous

Table 1 Chemical compositions of main components of nickel laterite ore (wt.%)

Ni	TFe	Fe_2O_3	Cr_2O_3	SiO_2
2.26	14.24	20	1.99	41.41

MgO	Al_2O_3	CaO	Mn
17.24	1.99	0.26	0.24

Table 2 Chemical phases and distribution of nickel in laterite ore

Constituent	Content/wt.%	Occupancy/%
Nickel silicate	1.93	85.4
Nickel sulfide	0.259	11.46
Adsorbed nickel	0.071	3.14
Total nickel	2.26	100

Fig. 1 XRD pattern of nickel laterite ore

serpentine $(Mg,Fe,Ni)_3Si_2O_5(OH)_4$, olivine $((Mg,Fe,Ni)_2SiO_4)$ and quartz (SiO_2), as well as hematite (Fe_2O_3), talc $(Mg_3(Si_4O_{10})(OH)_2)$, kaolinite $(Al_4[Si_4O_{10}](OH)_8)$, and chlorite $((Mg,Fe)_3[Si_4O_{10}]-(OH)_2\cdot(Mg,Fe)_3(OH)_6)$ as minor phases. The chemical analysis of coal (as the reductant) is given in Table 3.

Table 3 Chemical compositions of coal (wt.%)

Fixed carbon	Volatile matter	Ash	Moisture	P	S
67.83	18.45	12.02	1.48	0.003	0.022

The chemical analysis results (Table 3) of coal reveals that it was composed of 67.83% fixed carbon, 18.45% volatile matters, and 12.02% ash with a negligible trace of phosphorous and sulfur. The ore and coal were both crushed by passing a 2 mm laboratory roll crusher.

To examine the thermodynamic parameters of the deep reduction process of laterite nickel ores, the STA409CD synchronous thermal analyzer was used in this experiment [20]. Each sample weighed 30 mg, the full range of the synchronous thermal analyzer was 20 mV, and the heating rate was 10 °C/min. At temperatures of 20−1400 °C, the samples were analyzed on the synchronous thermal analyzer in air atmosphere, as shown in Fig. 2. As a result of endothermic and exothermic processes, two main peaks were observed on the differential scanning calorimeter (DSC) curve. The exothermic peak at 556.8 °C may be attributed to the formation of an amorphous phase by the removal of crystal water from kaolinite, serpentine and chlorite. The second intense exothermic peak at 827.5 °C was primarily caused by the heating recrystallization of minerals such as kaolinite, chlorite (primarily magnesium-rich species), and montmorillonite, and amorphous Mg_2SiO_4 crystallization after serpentine dehydroxylation. The laterite nickel ore had an endothermic peak at 1359.7 °C, which was the melting point of the studied low-grade laterite nickel ore, and the ore began to melt at this temperature. Three large mass loss values were presented by the TG curve in different temperature ranges of 25−150, 150−400 and 400−830 °C, corresponding to the removal of adsorption water, removal of crystal water, and recrystallization of amorphous mineral, respectively. The mass increase was primarily owing to the iron matter overflowing

from the lattice of the silicate minerals after recrystallization and then oxidized to hematite by O_2 in the air. The first main peak at 556.8 °C was caused by the removal of crystallized water from lizardite, corresponding to a mass loss of 9.6%. Furthermore, lizardite was decomposed to form an amorphous magnesium silicate phase.
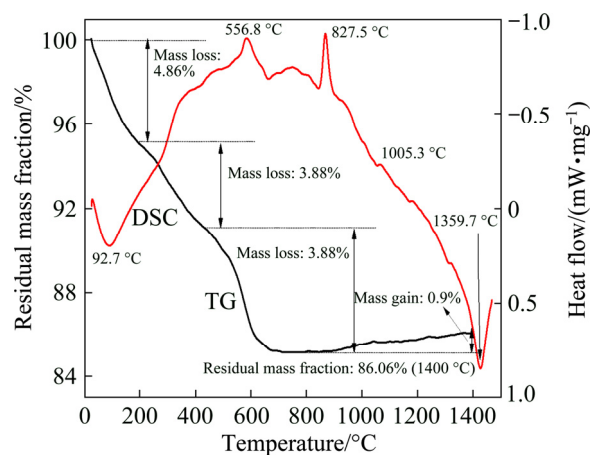

Fig. 2 TG−DSC curves of nickel laterite ores

2.2 Methods and equipment

The main parameters affecting deep reduction are reduction temperature, reduction time, mole ratio of fixed carbon to reducible oxygen, and CaO content. Four groups of experiments were designed to investigate the effects of these factors on Ni−Fe recovery.

To satisfy the feed size requirement of the experimental grinding equipment and the size required for the deep reduction test, the ore sample and reducing agent coal sample were crushed to <2 mm using jaw and roll crushers. The reduction equipment used in the deep reduction test was a self-designed one-way heating furnace. Its constant temperature zone length was 900 mm, the heating rate could reach 20 K/min, the working temperature could reach 1873 K, and the temperature control system was a programmable control cabinet. The schematic diagram of the one-way heating furnace used is shown in Fig. 3. In the deep reduction test, the crushed ore sample, pulverize coal and CaO were mixed in the preset proportion evenly, and 500 g of mixed sample was weighed and placed into a steel crucible. When the temperature in the furnace reached the preset temperature, the crucible was quickly placed into the furnace. After the temperature increased to the preset temperature, the reduction was started and the temperature was
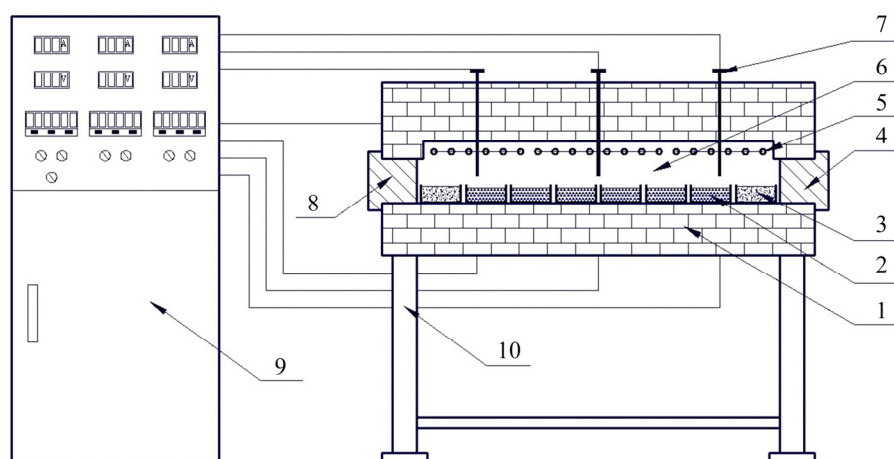
Fig. 3 Schematic diagram of reduction apparatus: 1—Furnace; 2—Prepared mixtures; 3—Coal; 4—Outlet; 5—MoSi$_2$ heating element; 6—Hearth; 7—Thermocouple for temperature measurement; 8—Inlet; 9—Control cabinet; 10—Bed

maintained. After the setting time, the raw material was quickly removed and quenched into water. After the material was cooled, it was placed in an oven for drying. Because the reduction furnace was a non-closed system, to maintain the reduction atmosphere in the chamber during deep reduction, protective coal was added at both ends of the furnace to protect the samples from oxidation.

A representative sample weighing 15 g obtained from each of the reduced products was wet ground in an XMB (d65 min × 76 mm) rod mill at a pulp density of 70 wt.%, constituting 85% passing 74 μm. The slurry was then separated through a CXG-φ50 magnetic tube with the magnetic field strength of 100 kA/m. The nickel and iron contents of the magnetic concentrate were determined by chemical analysis, and the recoveries were deduced according to mass balance.

The mineral compositions of both the reduced materials (under optimum reduction conditions) and magnetic concentrate were investigated by XRD (PANalytical B. V. PW3040/60) with Cu K$_\alpha$ radiation (40 kV, 40 mA) at the scanning rate of 12 (°)/min from 10° to 80°. The morphology and microstructure of the products above were studied using SEM on an SSX−550 scanning electron microscope produced by Shimadzu. Meanwhile, composition analysis was performed using EDS on an Inca X-ray spectrometer combined with a scanning electron microscope.

The carbon-containing coefficient was determined by oxygen content in iron (nickel) oxide. The oxygen content in iron oxide (nickel) could be expressed by

$$\beta_O = \beta_{TFe} \times 48/112 + \beta_{Ni} \times 16/59 \qquad (1)$$

where β_O is the oxygen content in raw ore; β_{TFe} is the total iron content in raw ore; β_{Ni} is the Ni content in raw ore.

It was noteworthy that only fixed carbon in coal and CO produced by gasification were assumed to have participated in the reduction reaction, while methane, hydrogen, and other hydrocarbons in volatile matter were not considered. In this study, the ratio of carbon in pulverized coal to oxygen in laterite nickel ore was used. A carbon-containing coefficient of 1 indicated the fixed carbon consumption when all iron (nickel) oxides in the laterite nickel ore were reduced to metal iron (nickel).

3 Results and discussion

A large number of studies have proven that for laterite nickel ores with high silicon and magnesium content, nickel exists as an independent mineral in the lattice of silicate minerals, e.g., serpentine is in an isomorphism of magnesium and iron. Therefore, it is difficult to enrich nickel in laterite nickel ores by physical mineral processing. Because the radii of iron and nickel atoms are similar, they can form a solid solution easily. Therefore, the nickel produced by deep reduction can be aggregated with relatively high content of iron as a carrier, and nickel can be enriched by magnetic separation from nonmagnetic gangue minerals.

3.1 Deep reduction test

3.1.1 Effect of reduction temperature

In deep reduction, the reduction temperature significantly affects product quality. Therefore, to investigate the effect of different reduction temperatures on the products of subsequent magnetic separation, under the conditions of reduction time 50 min, slag basicity 1.0, carbon-containing coefficient 2.5, and magnetic field strength 72 kA/m, the effect of reduction temperature on the deep reduction process was investigated. The relationships among nickel and iron grade, recovery of nickel–iron concentrate, and deep reduction temperature are shown in Fig. 4.
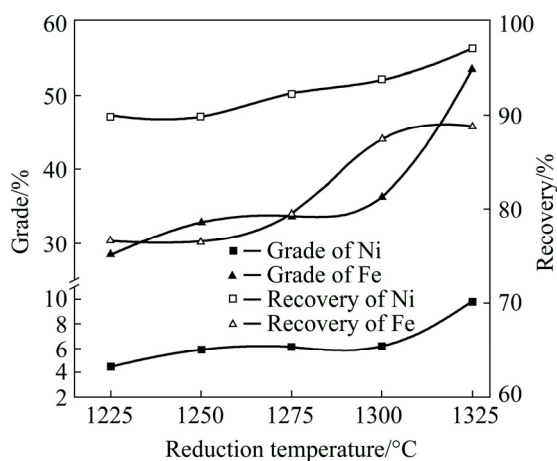

Fig. 4 Effect of reduction temperature on grades and recoveries of nickel and iron (reduction time 50 min, slag basicity of slag 1.0, carbon-containing coefficient 2.5, and magnetic field strength 72 kA/m)

To determine the effect of reduction temperature, low-grade laterite nickel ores were reduced at different temperatures from 1225 to 1325 °C, while other technological parameters remain unchanged. When the reduction temperature was increased from 1225 to 1325 °C, the nickel grade and recovery increased from 4.50% to 9.81% and 89.82% to 97.01%, respectively. With respect to the iron grade and recovery, the iron grade increased from 28.46% to 33.70% when the temperature was varied from 1225 to 1275 °C; however, a further increase in reduction temperature resulted in little change in nickel content. It is clear that increasing the temperature was beneficial to the deep reduction process. However, when the temperature was too high, the deep reduction material could bond and block easily. Considering the test conditions and energy factors, the test

temperature should be 1275 °C.

3.1.2 Effect of reduction time

Reduction time is an important factor in the deep reduction process of laterite nickel ores. Under the conditions of reduction temperature 1275 °C, slag basicity 1.0, carbon-containing coefficient 2.5, and magnetic field strength 72 kA/m, the effect of reduction time on the results of deep reduction and magnetic separation was examined. The experimental results are shown in Fig. 5.
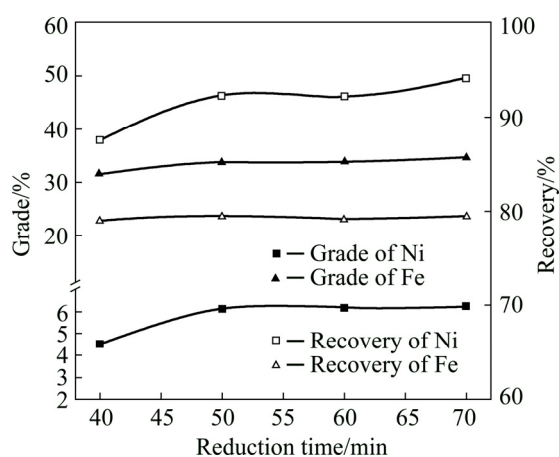

Fig. 5 Effect of reduction time on grades and recoveries of nickel and iron (reduction temperature 1275 °C, slag basicity 1.0, carbon-containing coefficient 2.5, and magnetic field strength 72 kA/m)

As shown in Fig. 5, the grade and recovery of nickel and iron in concentrate increased gradually from 40 to 70 min, but the increase in nickel and iron grade and the recovery of concentrate was not obvious when the reduction time was extended to 50 min. The main reason was that with the extension of reduction time, the reducing agent was gradually consumed, the reducing atmosphere in the furnace was gradually weakened, and the oxidizing atmosphere appeared locally, such that the reduced ore was reoxidized, thereby affecting the quality of the concentrate products. A long reduction time would also affect the processing capacity of the equipment, reduce production, and increase process energy consumption, which were economically unreasonable. Therefore, the deep reduction time was determined to be 50 min.

3.1.3 Effect of carbon

As an effective measure to improve the reduction rate, carbon has been applied in many metal reduction processes. Under the condition of reduction temperature 1275 °C, deep reduction time

50 min, slag basicity 1.0, and magnetic field strength 72 kA/m, the effect of carbon addition on the grade and recovery of nickel and iron from magnetic separation products was investigated. The carbon-containing coefficient was selected at six levels of 1.0, 1.5, 2.0, 2.5, 3.0 and 3.5, and the required coal was 7.30, 10.95, 14.60, 18.25, 21.90, and 25.55 wt.% of the raw ore, respectively. The results are shown in Fig. 6.
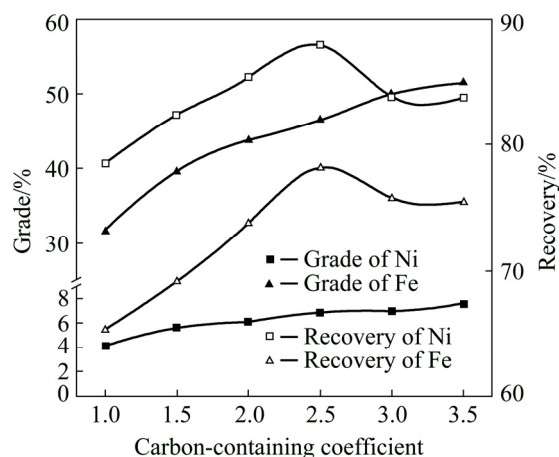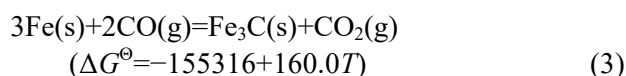

Fig. 6 Effect of carbon addition on grades and recoveries of nickel and iron (reduction temperature 1275 °C, slag basicity 1.0, deep reduction time 50 min, and magnetic field strength 72 kA/m)

As shown in Fig. 6, the recoveries of nickel and iron increased with the carbon-containing coefficient when the carbon-containing coefficient was less than 2.5, while they decreased when the carbon-containing coefficient increased beyond 2.5, which was primarily owing to the close contact between the reducing agent carbon particles and the mineral powder particles, and the uniform distribution of carbon increasing the effective surface area of the reaction. Meanwhile, because carbon consumption increased the porosity of the material, the intermediate products CO (CO_2) could react with the nearby metal oxides (carbon) immediately, such that the reduction could proceed faster. When the carbon-containing coefficient was large, the unreacted residual carbon could hinder the diffusion and condensation of nickel and iron particles, resulting in an incomplete reduction of laterite nickel ores. Furthermore, the excessive carbon-containing coefficient at high temperatures could accelerate the reduction of ferrocarburizing, resulting in cementite formation (Eqs. (2) and (3)), thereby reducing the metallization rate of reduced

ores.

$$3Fe(s)+C(s)=Fe_3C(s) \quad (\Delta G^\ominus=11234-11.0T) \quad (2)$$

$$3Fe(s)+2CO(g)=Fe_3C(s)+CO_2(g)$$
$$(\Delta G^\ominus=-155316+160.0T) \quad (3)$$

Therefore, when coal was used as a reducing agent to reduce laterite nickel ores, the carbon-containing coefficient should be significantly higher than the theoretical value to obtain a better reduction and separation. However, the excessive carbon-containing coefficient not only reduced the reduction and separation, but also caused high energy consumption. Therefore, the carbon-containing coefficient of the subsequent test was determined to be 2.5.

3.1.4 Effect of slag basicity

Among the methods to strengthen the reduction and separation of laterite nickel ores, adding appropriate additives is considered to be the most effective method, and extensive studies have been performed accordingly [21]. The acidity−basicity index of slag is called the slag basicity (R). Slag basicity is typically expressed by the ratio of the mass percentage of alkaline oxides to acid oxides in slag, which can be expressed in the following three formulas: $R=w(CaO+MgO)/w(SiO_2+Al_2O_3)$ is called the quaternary slag basicity, also called the total slag basicity; $R=w(CaO+MgO)/w(SiO_2)$ is the ternary slag basicity; $R=w(CaO)/w(SiO_2)$ is the binary basicity. In this study, the quaternary slag basicity was selected as the influencing factor. Slag basicity significantly affected the ironmaking process and hence the deep reduction process. Therefore, under the conditions of reduction temperature 1275 °C, reduction time 50 min, carbon-containing coefficient 2.5 and magnetic field strength 72 kA/m, slag basicity was adjusted by adding different amounts of analytical pure CaO, and the effect of slag basicity on the deep reduction process was investigated. The experimental results are shown in Fig. 7.

Figure 7 indicates that when the slag basicity was less than 1.0, the iron recovery of the concentrate increased with the increase of slag basicity; when the slag basicity exceeded 1.0, the iron recovery of concentrate decreased with the increase in slag basicity, which was primarily because the slag basicity affected the slag composition in the deep reduction process. Iron oxides were displaced from fayalite ($2FeO·SiO_2$)
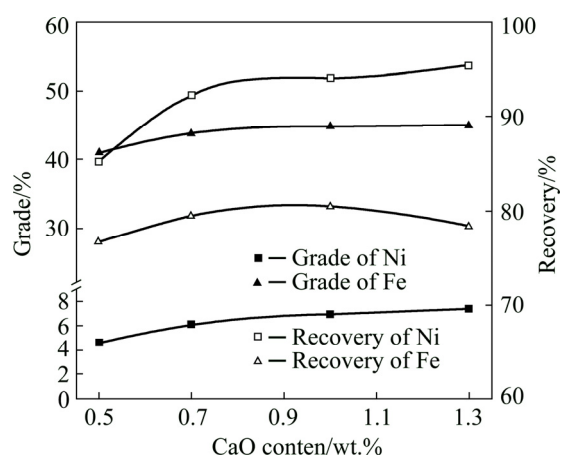
Fig. 7 Effect of CaO content on grades and recoveries of nickel and iron (reduction temperature 1275 °C, reduction time 50 min, carbon-containing coefficient 2.5, and magnetic field strength 72 kA/m)

owing to the addition of CaO, which affected the spilling and enriching rate of iron from silicate minerals to form nickel–iron particles in the deep reduction process. Therefore, the slag basicity should be 1.0. Under these conditions, the nickel concentrate with nickel grade 6.96%, nickel recovery 94.06%, iron grade 34.74%, and iron recovery 80.44% could be obtained.

3.2 Mechanism analysis

3.2.1 Mechanism analysis of reduction process

The reaction characteristics of laterite nickel ores were studied under the same batching scheme. The effects of reduction temperature on the deep reduction process were discussed by studying the differences in chemical composition, mineral composition, and micro-morphology of reduced materials at different reduction temperatures. The XRD spectra of the reduced materials at different reduction temperatures are shown in Fig. 8.

As shown in Fig. 8, with the increase in reduction temperature, the diffraction peaks of ferronickel increased gradually, while those of olivine decreased gradually. It can be inferred that
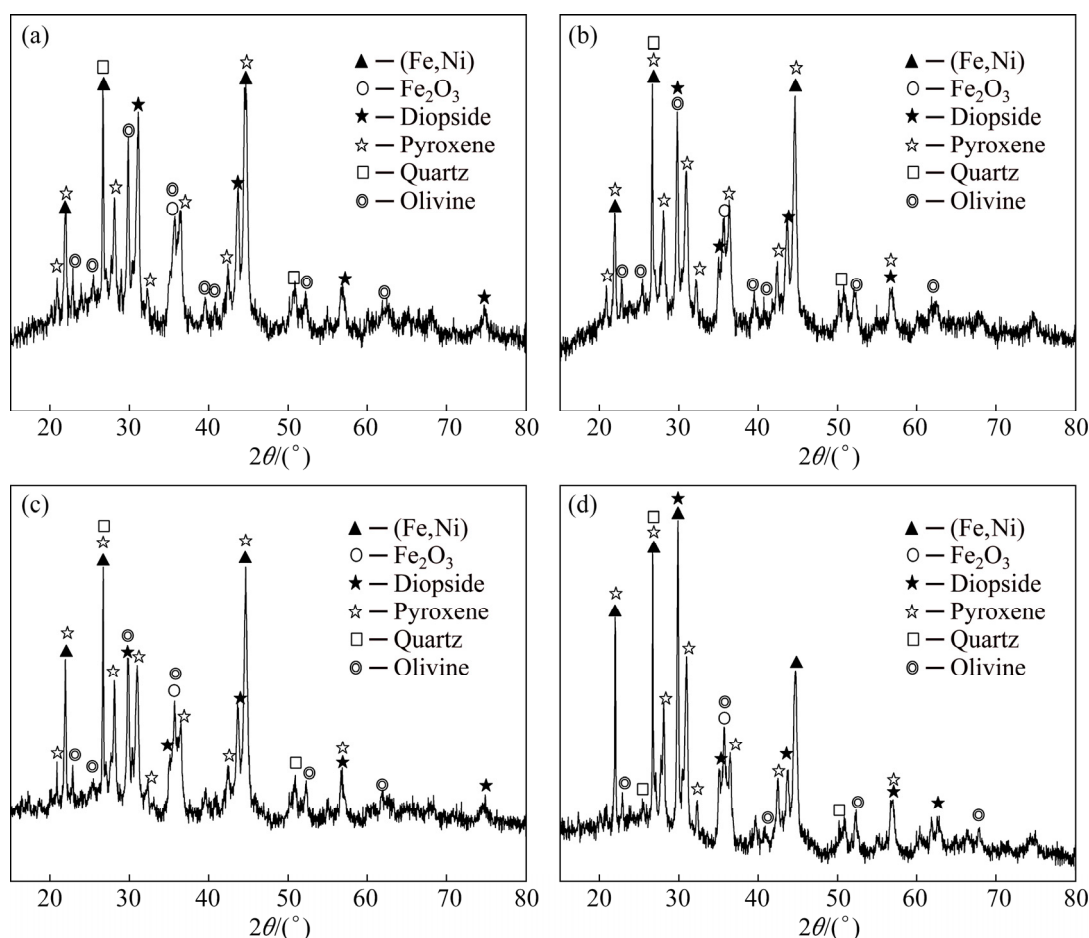

Fig. 8 XRD patterns of deoxidized samples at different deoxidization temperatures: (a) 1250 °C; (b) 1275 °C; (c) 1300 °C; (d) 1325 °C

the content of nickel–iron particles from olivine increased gradually. Meanwhile, the diffraction peaks of refractory pyroxene, diopside, and quartz increased gradually. It can be inferred that increasing the temperature would accelerate the reduction of iron (nickel) oxides and increase the contents of nickel and iron, while the side effects would be aggravated and the reduction of impurity elements (such as Si, Al) may be increased.

The SEM images of the reduced materials at different temperatures are shown in Fig. 9. As shown in Fig. 9(a), at some points of the laterite nickel ore, nickel–iron could react with CO produced by coal powder in air to form a small amount of nickel–iron particles, which existed on the surface of the matrix in the form of tiny irregular particles. When the reduction temperature increased, the irregular particles grew gradually (Figs. 9(b, c)) and spherical and similar spherical particles formed from the matrix. Subsequently, the particles precipitated and fell off into the nickel–iron particles (Fig. 9(c)). With the increase in reduction temperature, the Ni−Fe particles that precipitated from the matrix were embedded in the molten gangue minerals (Fig. 9(d)). Therefore, in a certain range, increasing the reduction temperature was conducive to the enrichment and growth of nickel–iron particles and the promotion of reaction;

however, an excessively high temperature would melt gangue minerals, bond nickel–iron particles formed by deep reduction, increase the reduction of impurity elements, and reduce the quality of reduction products, which were not conducive to the separation of nickel–iron particles and gangue minerals. Therefore, the temperature for deep reduction should not only ensure the enrichment of ferronickel to form ferronickel particles, but also limit the process temperature; otherwise, the process would fail completely.

3.2.2 Mechanism analysis of magnetic separation process

To determine the useful components and impurity content of the ferronickel concentrate obtained by magnetic separation, chemical multi-element and XRD analyses were performed on the concentrate products. The results are shown in Table 4, Table 5 and Fig. 10.

As shown in Table 4, Table 5 and Fig. 10, nickel and iron were effectively enriched, and impurities such as olivine were effectively reduced by magnetic separation. In addition, Table 4 shows that the S and P contents of the concentrate were lower than those of the tailing, which demonstrates that the reduction material could yield good dephosphorization and desulfurization effects by magnetic separation.
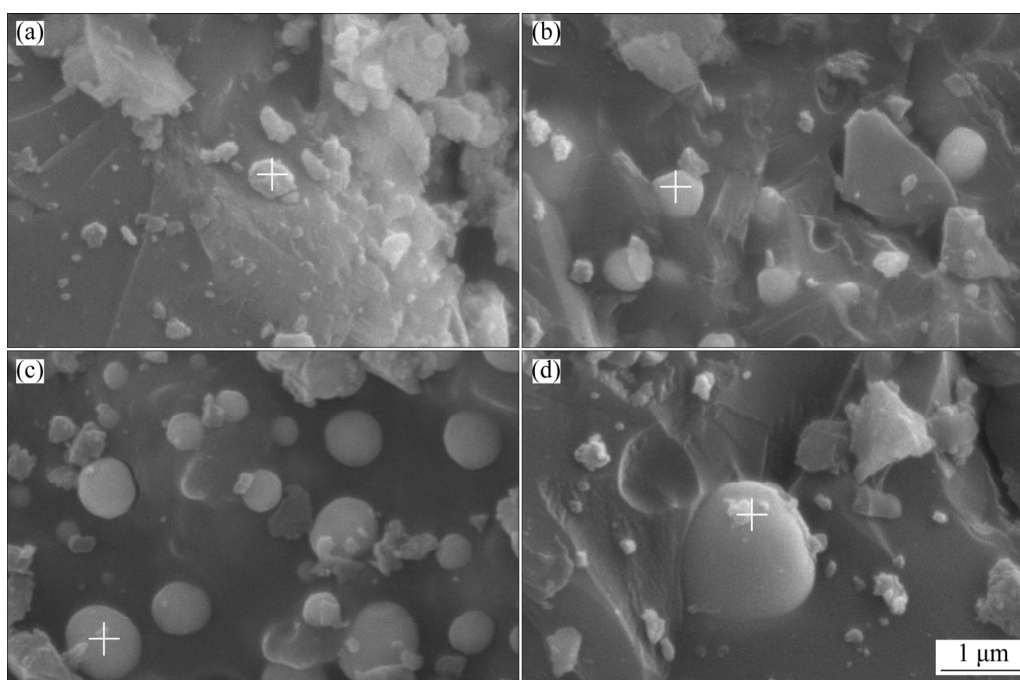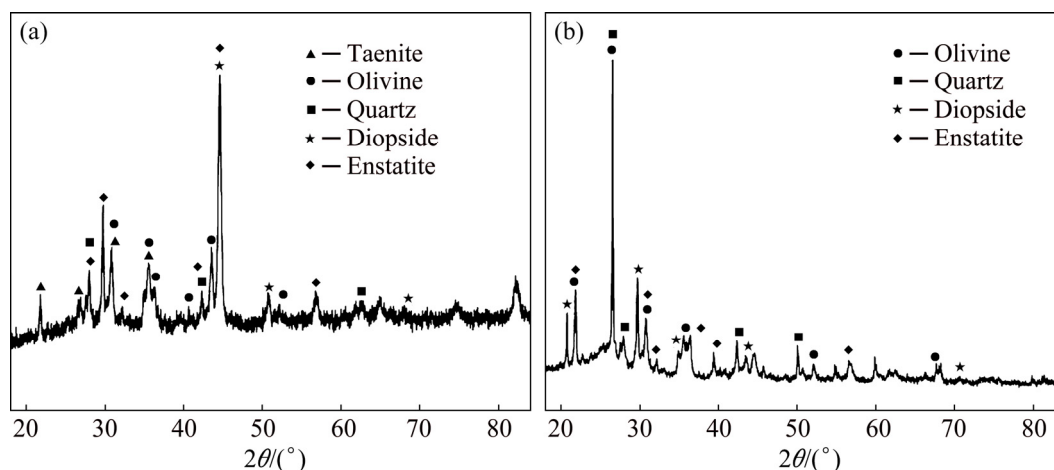

Fig. 9 SEM images of reduced materials at different deoxidization temperatures (reduction time 50 min, slag basicity 1.0, carbon-containing coefficient 2.5): (a) 1250 °C; (b) 1270 °C; (c) 1300 °C; (d) 1325 °C

Table 4 Chemical compositions of magnetic separation products (wt.%)

Product	TFe	Ni	SiO$_2$	MgO	Al$_2$O$_3$	CaO	C	S	P
Concentrate	34.74	6.96	34.26	13.82	2.56	5.27	0.32	0.011	0.002
Tailing	6.70	0.34	44.06	11.78	3.66	5.56	22.4	0.29	0.006

Table 5 Results of magnetic separation

Constituent	Yield/%	Grade/%		Recovery/%	
		Ni	Fe	Ni	Fe
Concentrate	42.88	6.96	34.74	94.06	80.44
Tailing	57.12	0.34	6.70	5.94	19.56
Feed ore	100.00	2.26	14.24	100.00	100.00

Fig. 10 XRD patterns of magnetic separation products: (a) Concentrate; (b) Tailing

The SEM image and EDS energy spectrum of the concentrate obtained by magnetic separation are shown in Figs. 11(a) and (b), respectively. Figure 11(a) shows that the concentrate adhered to the surface of the gray matrix by extremely fine, bright white particles (shown by Point 1). The matrix was primarily composed of magnesium silicate minerals composed of Si, Mg, Ca and other elements. The bright white particles contained certain nickel and iron components. These nickel and iron particles existed in the interior of the laterite nickel ores. Because the amount of CO gas entering the reaction layer was insufficient, the reduction was incomplete, where only nickel–iron particles of a smaller size were formed. If the reduction time was further prolonged, the larger nickel–iron particles on the surface of the laterite nickel ore would be oxidized; if the deep reduction time was long, the hot agglomeration of metal nickel–iron particles would occur, which was not conducive to the operation of burden. However, this part of the material could be used as a good nucleating agent to promote the deep reduction process.

The SEM image and EDS energy spectrum of the tailing obtained by magnetic separation are shown in Figs. 11(c) and (d), respectively. As shown (under the conditions of reduction temperature 1275 °C, reduction time 50 min, slag basicity 1.0, carbon-containing coefficient 2.5, and magnetic field strength 100 kA/m), after the deep reduction and magnetic separation of the laterite nickel ores, the metallic nickel–iron particles on the gangue matrix (shown by Point 2) fell off automatically and small circular pits remained, indicating that the mosaic force of the nickel–iron particles in the gangue matrix was relatively small; therefore, a simple grinding could dissociate the nickel–iron particles from the mosaic. Meanwhile, the nonmagnetic products were primarily silicate minerals, indicating that the concentrates of nickel and iron were well enriched.
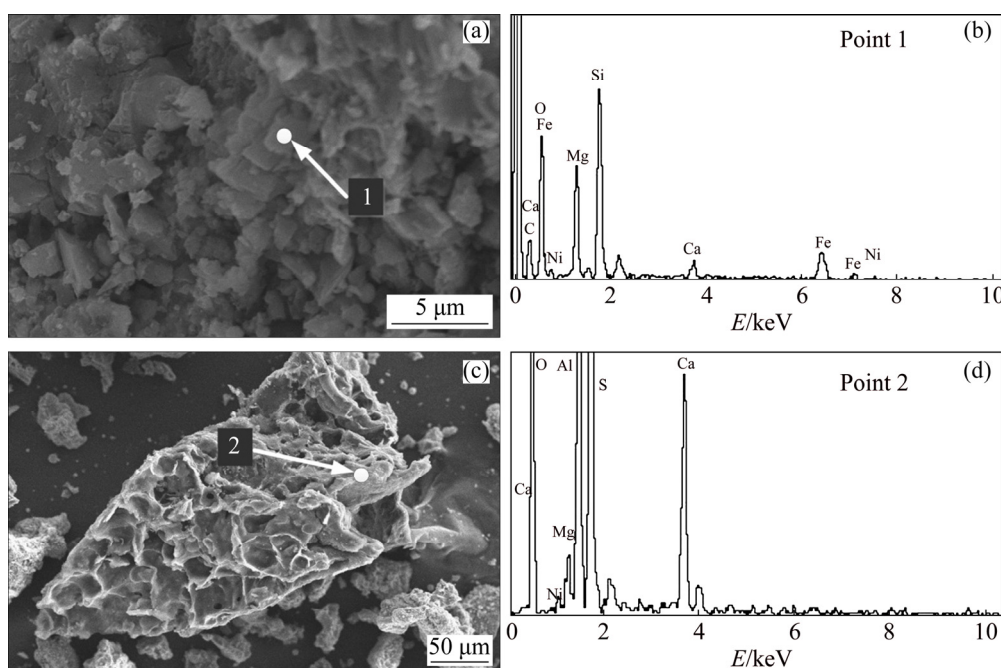
Fig. 11 SEM images (a, c) and EDS spectra (b, d) of concentrate (a, b) and tailing (c, d) after magnetic separation

4 Conclusions

(1) From the deep reduction and magnetic separation tests, the deep reduction material was obtained under the conditions of reduction temperature 1275 °C, reduction time 50 min, slag basicity 1.0, and carbon-containing coefficient 2.5. A nickel–iron concentrate with nickel grade 6.96%, nickel recovery 94.06%, iron grade 34.74%, and iron recovery 80.44% could be obtained by magnetic separation with magnetic field strength of 72 kA/m.

(2) The mechanisms of deep reduction and magnetic separation demonstrated that the reduction temperature and time affected the possibility and reaction progress of deep reduction. Slag basicity affected the composition of slag in the furnace and the overflowing and enriching rate of nickel–iron from the matrix to form nickel–iron particles. During the deep reduction reaction, nickel–iron particles formed, aggregated, and grew gradually. The separation of nickel–iron ores from gangue minerals could be effectively promoted by magnetic separation.

References

[1] YANG Wan-peng, LI Jia-rong, LIU Shi-zhong, SHI Zhen-xue, ZHAO Jin-qian, WANG Xiao-guang. Orientation dependence of transverse tensile properties of nickel-based third generation single crystal superalloy DD9 from 760 to 1100 °C [J]. Transactions of Nonferrous Metals Society of China, 2019, 29(3): 558−568.

[2] MU Wen-ning, LU Xiu-yuan, CUI Fu-hui, LUO Shao-hua, ZHAI Yu-chun. Transformation and leaching kinetics of silicon from low-grade nickel laterite ore by pre-roasting and alkaline leaching process [J]. Transactions of Nonferrous Metals Society of China, 2018, 28(1): 169−176.

[3] FAN Su-feng, ZHANG Tao, YU Kun, FANG Hong-jie, XIONG Han-qing, DAI Yi-long, MA Jia-ji, JIANG Da-yue, ZHU Hua-long. Compressive properties and energy absorption characteristics of open-cell nickel foams [J]. Transactions of Nonferrous Metals Society of China, 2017, 27(1): 117−124.

[4] DONG Jing-cheng, WEI Yong-gang, ZHOU Shi-wei, LI Bo, YANG Yin-dong. The effect of additives on extraction of Ni, Fe and Co from nickel laterite ores [J]. JOM, 2018, 7(17): 2365−2377.

[5] MORCALI M H, KHAJAVI L T, DREISINGER D B. Extraction of nickel and cobalt from nickeliferous limonitic laterite ore using borax containing slags [J]. International Journal of Mineral Processing, 2017, 167: 27−34.

[6] KURSUNOGLU S, ICHLAS Z T, KAYA M. Dissolution of lateritic nickel ore using ascorbic acid as synergistic reagent in sulphuric acid solution [J]. Transactions of Nonferrous Metals Society of China, 2018, 28(8): 1652−1659.

[7] LI Jin-hui, CHEN Zhi-feng, SHEN Bang-po, XU Zhi-feng, ZHANG Yun-fang. The extraction of valuable metals and phase transformation and formation mechanism in roasting-water leaching process of laterite with ammonium sulfate [J]. Journal of Cleaner Production, 2017, 140: 1148−1155.

[8] MACCARTHY J, NOSRATI A, SKINNER W, ADDAI-

MENSAH J. Atmospheric acid leaching mechanisms and kinetics and rheological studies of a low grade saprolitic nickel laterite ore [J]. Hydrometallurgy, 2016, 160: 26−37.

[9]   LI Guang-hui, SHI Tang-ming, RAO Ming-jun, JIANG Tao, ZHANG Yuan-bo. Beneficiation of nickeliferous laterite by reduction roasting in the presence of sodium sulfate [J]. Minerals Engineering, 2012, 32: 19−26.

[10]   LE L, TANG J, RYAN D, VALIX M. Bioleaching nickel laterite ores using mult-metal tolerant *Aspergillus foetidus* organism [J]. Minerals Engineering, 2006, 19: 1259−1265.

[11]   MCDONALD R G, WHITTINGTON B I. Atmospheric acid leaching of nickel laterites review. Part II: Chloride and bio-technologies [J]. Hydrometallurgy, 2008, 91: 56−69.

[12]   LI Bo, WANG Hua, WEI Yong-gang. The reduction of nickel from low-grade nickel laterite ore using a solid-state deoxidisation method [J]. Minerals Engineering, 2011, 24: 1556−1562.

[13]   FARROKHPAY S, FILIPPOV L. Challenges in processing nickel laterite ores by flotation [J]. International Journal of Mineral Processing, 2016, 151: 59−67.

[14]   ZHU D Q, CUI Y, VINING K, HAPUGODDA S, DOUGLAS J, PAN J. Upgrading low nickel content laterite ores using selective reduction followed by magnetic separation [J]. International Journal of Mineral Processing, 2012, 106: 1−7.

[15]   WANG Lun-wei, LV Xue-ming, LIU Mei, YOU Zhi-xiong, LV Xue-wei, BAI Chen-guang. Preparation of ferronickel from nickel laterite via coal-based reduction followed by magnetic separation [J]. International Journal of Minerals, Metallurgy, and Materials, 2018, 25(7): 744−751.

[16]   TANG Xiao-hui, LIU Run-zao, LI Yao, JI Zhi-jun, ZHANG Yan-ting, LI Shi-qi. Ferronickel enrichment by fine particle reduction and magnetic separation from nickel laterite ore [J]. International Journal of Minerals, Metallurgy, and Materials, 2014, 21(10): 955−961.

[17]   RAO Ming-jun, LI Guang-hui, ZHANG Xin, LUO Jun, PENG Zhi-wei, JIANG Tao. Reductive roasting of nickel laterite ore with sodium sulfate for Fe−Ni production. Part II: Phase transformation and grain growth [J]. Separation Science & Technology, 2016, 51(10): 1−9.

[18]   WANG Xiao-ping, SUN Ti-chang, CHEN Chao, KOU Jue. Effects of Na_2SO_4 on iron and nickel reduction in a high-iron and low-nickel laterite ore [J]. International Journal of Minerals, Metallurgy and Materials, 2018, 25(4): 383−390.

[19]   SUN Yong-sheng, ZHOU Wen-tao, HAN Yue-xin, LI Yan-jun. Effect of different additives on reaction characteristics of fluorapatite during coal-based reduction of iron ore [J]. Metals, 2019, 9(9): 923−943.

[20]   HARJANTO S. RHAMDHANI M A. Sulfides formation in carbothermic reduction of saprolitic nickel laterite ore using low-rank coals and additives: A thermodynamic simulation analysis [J]. Minerals, 2019, 9(10): 631−652.

[21]   PAN Jian, ZHENG Guo-lin, ZHU De-qing, ZHOU Xian-lin. Utilization of nickel slag using selective reduction followed by magnetic separation [J]. Transactions of Nonferrous Metals Society of China, 2013, 23(11): 3421−3427.

红土镍矿深度还原−磁选工艺富集镍和铁

袁 帅，周文涛，李艳军，韩跃新

东北大学 资源与土木工程学院，沈阳 110819

摘　要：提出采用"深度还原−磁选"工艺从红土镍矿中富集镍和铁。结果表明，在还原温度 1275 ℃、还原时间 50 min、渣相碱度 1.0、配碳系数 2.5 和磁场强度 72 kA/m 的条件下，可得到镍品位为 6.96%、回收率为 94.06% 和 铁品位为 34.74%、回收率为 80.44% 的镍铁精矿产品。分析表明，还原温度和时间影响深度还原发生的可能性及 反应进度，渣相碱度影响炉料中渣的组成及镍铁元素从基体中溢出富集形成镍铁颗粒的速度，深度还原反应过程 中镍铁颗粒生成、聚集并逐渐长大，经磁选后可有效促进镍铁矿物与脉石矿物分离。
关键词：红土镍矿；深度还原；磁选；镍铁精矿；还原机制

(Edited by Bing YANG)